MODELLING STRATEGIES FOR TRADITIONAL EARTHQUAKE RESISTANT SOLUTIONS ENHANCING WALL-TO-WALL CONNECTIONS

Antonio Murano[1], Javier Ortega[2], Graça Vasconcelos[3], Hugo Rodrigues[4]

1: ISISE, School or Engineering, University of Minho (Campus de Azurem)
e-mail: antoniomurano1987@gmail.com

2: ISISE, School or Engineering, University of Minho (Campus de Azurem)
e-mail: johe00@gmail.com

3: ISISE, School or Engineering, University of Minho (Campus de Azurem)
e-mail: graça@civil@uminho.pt

4: Polytechnic of Leiria, Department of Civil Engineering
e-mail: hugo.f.rodrigues@ipleiria.pt

Keywords: stone masonry, numerical modelling, modelling strategy, earthquake resistant techniques, out-of-plane behaviour

Abstract *Traditional masonry buildings located in seismic prone areas often present construction techniques empirically developed to improve the buildings seismic performance, for example by enhancing their box-behaviour in order to avoid premature out-of-plane failure of masonry walls. Often, earthquake-resistant techniques consist of a combination of locally available materials, such as timber or metal ties, embedded in masonry components.*

Finite Elements Macro-modelling approximates masonry as a homogeneous isotropic continuum, in order to obtain simpler and larger meshes, because the model does not have to describe the internal structure of masonry. One of the main challenges related to the numerical simulations is the use of adequate constitutive materials models able to replicate the non-linear behaviour of masonry. In the framework of macro-modelling approach of the masonry walls, an additional challenge is the modelling strategy to simulate the contribution of elements embedded in masonry, which work as traditional earthquake resistant solutions.

This work presents the results of the numerical analyses simulating the out-of-plane response of reduced scale (1:2) U-shaped stone masonry walls built with earthquake resistant techniques embedded at the corners, namely steel ties in wall 1 and timber lath beams in wall 2, which were tested experimentally.

The work primarily aims at the comparison of the results obtained with two different modelling strategies for the two reinforcing solutions, namely using 3D beams elements (CL18B) and solid elements (CHX60).

The outcomes provided by this work represent a useful contribution to achieve a deeper understanding regarding the consistency of the aforementioned strategies in capturing the influence of traditional of earthquake resistant techniques on the out-of-plane response of reinforced stone masonry walls.

1. INTRODUCTION

Earthquakes represent one of the major threat for masonry structures. Constructive flaws such as lack of effective connection among structural components and/or high percentage of voids can often result in out-of-plane failures.

In ancient times, traditional earthquake-resistant techniques were developed in seismic-prone areas with the aim of minimize the disadvantages of a specific natural environment. Locally available materials (e.g. timber) were embedded in load bearing elements in order to improve the box behaviour [1] [2]. In current building practice tying/anchoring systems are commonly used with the same purpose [3].

Out-of-plane behaviour of stone masonry walls has been intensively investigated both experimentally and numerically, but there is still a limited understanding of this phenomenon [4] [5] [6] [7].

Nowadays, FE methods is widely applied to perform structural analyses of masonry constructions [8]. Macro modelling and micro/meso modelling are the main FE-based approaches to model masonry structures [9]. This work focuses mainly on the former one (macro modelling) which can represent a good solution applicable also in practice-oriented engineering activities.

1.1. Objective and methodology of the present work

The present paper shows the comparison of two different modelling approaches in simulating the results of an experimental campaign aimed at the assessment of the out-of-plane performance of ston masonry walls built with earthquake-resistant techniques.

The experimental activities carried out are a further development of the work realized by Maccarini et al. (2018) [10] aiming at the characterization of the out-of-plane behaviour of unreinforced stone masonry walls.

Both unreinforced and reinforced reduced scale masonry walls were investigated by means of non-destructive testing, namely sonic tests and dynamic identification test, in order to estimate mechanical properties and natural frequency of vibration and calibrate the numerical models.

The numerical simulations presented in the following sections are based on a macro-modelling approach, which approximates the masonry as homogeneous anisotropic continuum. An additional challenge is represented by the selection of the most suitable strategy in order to accurately replicate the behaviour of reinforcing elements embedded in masonry components.

2. EXPERIMETAL RESULTS: OVERVIEW

The section present a summary related to the experimental activities carried out in order to characterize the tested specimens both from a geometrical and from a mechanical point of view. Therefore, the construction process of the stone masonry walls prototypes will be briefly described, as well as the non-destructive testing procedures applied in order to gather data for the calibration of the numerical models.

It is important to point out that the same geometrical parameters were used for unreinforced (WALL 0) and reinforced walls (WALL 1 and WALL 2). Additionally, their mechanical characterization was realized applying the same procedures. Finally, the prototypes herein described were built in a reduced scale (1:2).

2.1. Testing specimens and mechanica property assessment

The tested stone masonry walls prototypes have characteristics commonly found in vernacular buildings in northern Portugal [11]. U-shaped masonry walls specimens were adopted to study the connection between façade and lateral walls.

The majority of vernacular buildings in northern Portugal are usually limited to one floor. Moreover, specimen geometrical parameters were set according to the most recurring values detected in the reference area (Northern Portugal): wall span equal to 4.50 m; height of 2.70 m; thickness both for façade and lateral walls equal to 0.60 m. The same thickness (0.60 m) was assumed for the transversal walls, whose length was 2.0 m.

The walls were built roughly following a set of technical drawings indicating stone dimensions and position of the through stones. The masonry walls were laid on a reinforced concrete beam base (height equal to 20 cm); see Figure 1.

Figure 1. From left to right: WALL 0, WALL 1, WALL 2 construction phases

In WALL 1, steel elements were installed in both corners on top of the 3rd and 5th masonry layer. Steel reinforcing elements have a length equal to 0.70 m and a thickness equal to 4.50 mm. The ending parts of the steel ties (length equal to 45 mm), were bended downwards and inserted in holes drilled in the stones.

In WALL 2, timber lath beams were embedded within the corners of the wall in the same location selected for the steel braces. The length of the longitudinal element is 0.70 m. The cross-section dimensions of the timber members were 50X35 mm^2 for the longitudinal elements and 35X25 mm^2 for the transversal elements (Figure 2).
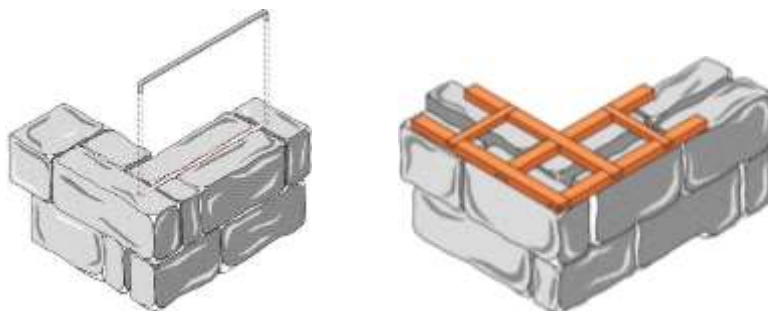
Figure 2. Steel reinforcements (left); Timber reinforcements (rigth)

Sonic tests have been carried out in order to estimate reference elastic mechanical properties to be implemented in the numerical models (see Table 1).

	Direct Sonic Tests V_P (m/s)			Indirect Sonic Tests V_P (m/s)			Indirect Sonic Tests V_R (m/s)			Poisson Ratio (v)	Young Mod. E (MPa)
	Mean	STD	CoV (%)	Mean	STD	CoV (%)	Mean	STD	CoV (%)	Mean	Mean
WALL 0	1955	230	12	-	-	-	-	-	-	0.39	4115
WALL 1	1381	209	13	1233	100	8	627	56	9	0.28	2960
WALL 2	1626	363	20	1270	77	6	693	40	6	0.25	3450

Table 1. Sonic tests results

Dynamic identification tests provided data regarding natural frequencies and mode shapes that can be used to calibrate the numerical models and adjust, if needed, the material properties (Table 2).

	Mode 1 (Hz)	Mode 2 (Hz)	Mode 3 (Hz)
WALL 0	26.70	-	-
WALL 1	20.60	31.25	41.80
WALL 2	21.29	31.25	45.22

Table 2. WALL 0, WALL 1, WALL 2 natural frequencies

2.2. Out-of-plane experimental behaviour

In order to perfrom the out-of plane test, an airbag (area of 1.65 X 1.35 square meters) was used to apply a uniform horizontal load to the frontal wall that simulates the seismic action. The airbag was installed on a supported steel frame. A vertical load of 10 kN, corresponding to a normal compressive load of approximately 0.05 MPa, was also applied to the transversal walls to simulate the self-weight of a timber roof.

Four load cells, placed between the steel profiles and the reaction wall at the level of the horizontal steel profiles, were used to record, the load applied by the airbag to the wall.

In order to avoid any possible sliding displacements, six steel posts were placed between the concrete base of the prototype and the laboratory reaction wall (Figure 3). Two steel posts were also placed at the back of the transversal walls between the concrete base and the reaction slab to avoid a possible overturning of the concrete base (Figure 3).
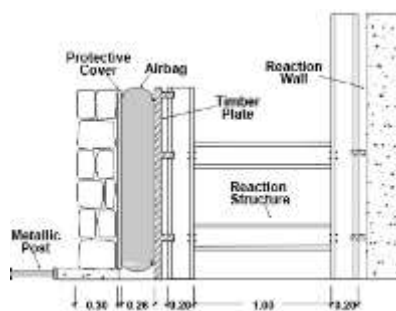
Figure 3. Out-of-plane test setup

The out-of-plane test was carried out under displacement control. The control point was located at the top of the frontal wall at its mid-span, where the highest displacement was

expected. The monitoring of the displacements of the frontal wall during the out-of-plane test was carried out using linear variable differential transducers (LVDTs). Sixteen monitoring points were set in the façade of the first prototype (steel reinforced wall), whereas 14 points were defined during the second test (timber reinforced wall). Moreover, 2 displacement transducers were placed in the transversal walls of the first prototype, in order to measure possible cracking and detachment of the frontal walls, whereas 4 displacement transducers were placed on the transversal walls of the second specimen to detect any possible detachments at the interface between timber and stone/mortar.

Figure 4 presents the results of the out-of-plane tests of WALL 0, WALL 1 and WALL 2. The force represents the sum of the values recorded by the four load cells. The displacement is representative of the control LVDT. The out-of-plane behaviour of WALL 1 and WALL 2 is similar in terms of maximum force values, with an elastic regime that lasts almost until peak load and a relatively smooth softening corresponding to the decrease of the force while increasing lateral displacements.
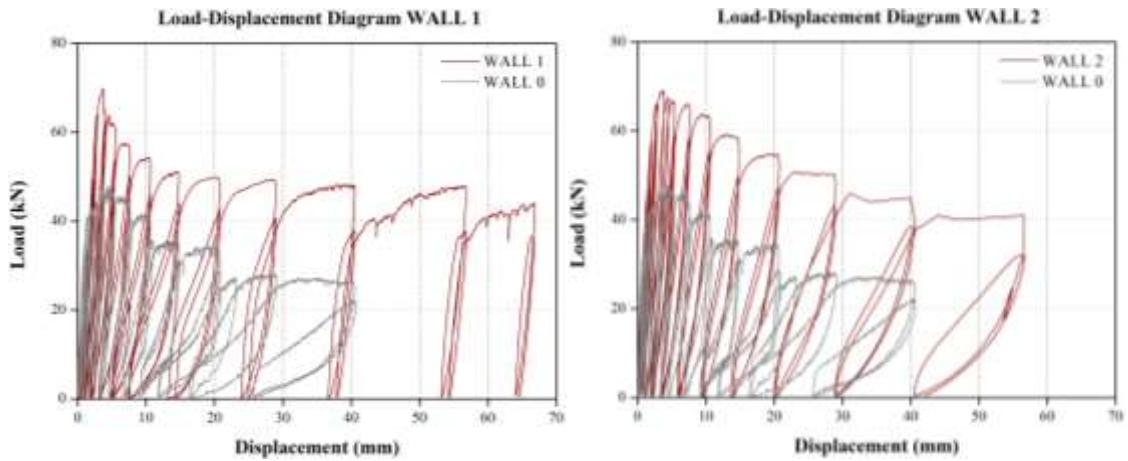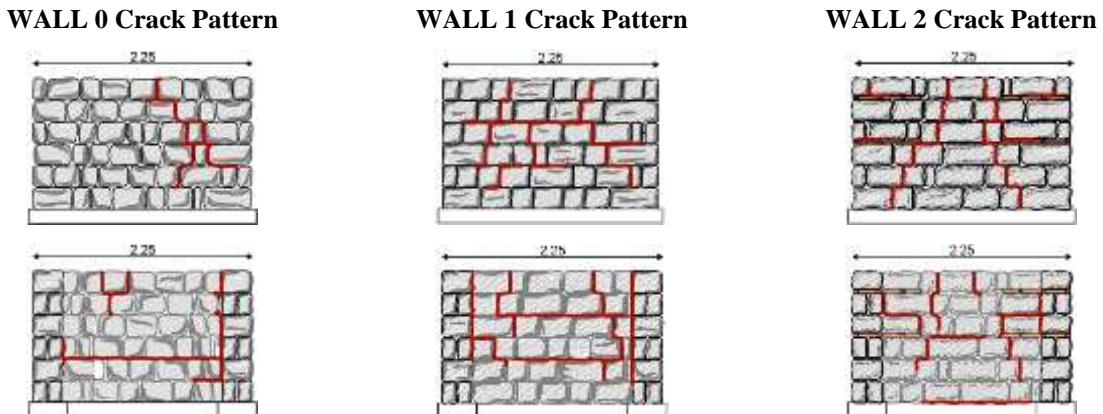

Figure 4. Load VS Displacements diagrams

Figure 5 depicts the final damage patterns observed in WALL 0, WALL 1 and WALL 2.

WALL 0 Crack Pattern	WALL 1 Crack Pattern	WALL 2 Crack Pattern

Figure 5. Crack patterns (WALL 0, WALL 1, WALL 2): front elevations (top) and rear elevations (bottom)

3. NUMERICAL SIMULATION

This section presents on one hand, a methodology aimed at the calibration of the numerical model with the experimental results, namely sonic tests, dynamic tests and out-of-plane test. On the other, two different modelling strategies will be compared to capture the behaviour of reinforcing elements. The out-of-plane test will be simulated by means of a static nonlinear analysis (pushover analysis) using DIANA software (TNO 2016) [12].

In all the analyses carried out, the material model adopted is a standard isotropic Total Strain Rotating Crack Model (TSRM) [12]. It is selected because of its robustness and simplicity, and because it is very well suited for analyses predominantly governed by cracking or crushing of the material [13] [14].

An exponential softening function simulates the non-linear behaviour of the material in tension, whereas the compressive function selected to model the crushing behaviour is parabolic [12].

Moreover, a linear elastic behaviour is assumed for the concrete base of the prototypes with a modulus of elasticity of 31 GPa and a Poisson's ratio of 0.2.

Steel Young modulus was assumed equal to 210000 MPa, whereas 7800 kg/m^3 and 0.3 are the selected values for density and Poisson ratio respectively. Timber Young modulus was assumed equal to 10000 MPa; timber density and Poisson ratio are equal to 600 kg/m3 and 0.20 respectively.

3.1. Finite Element model approaches

The numerical model of the wall was realized using twenty-node tetrahedron solid 3D elements (CHX60). The concrete base was also included in the numerical model using the same solid 3D elements. Plane quadrilateral interface elements (CQ48I) in a three-dimensional configuration were applied in order to reproduce the connection between the concrete base and the strong floor of the laboratory. Full connection was considered between the wall and the concrete base (Figure 6).

Mesh configuration WALL 0 **Mesh configuration WALL 1** **Mesh configuration WALL 2** **Base Interface**
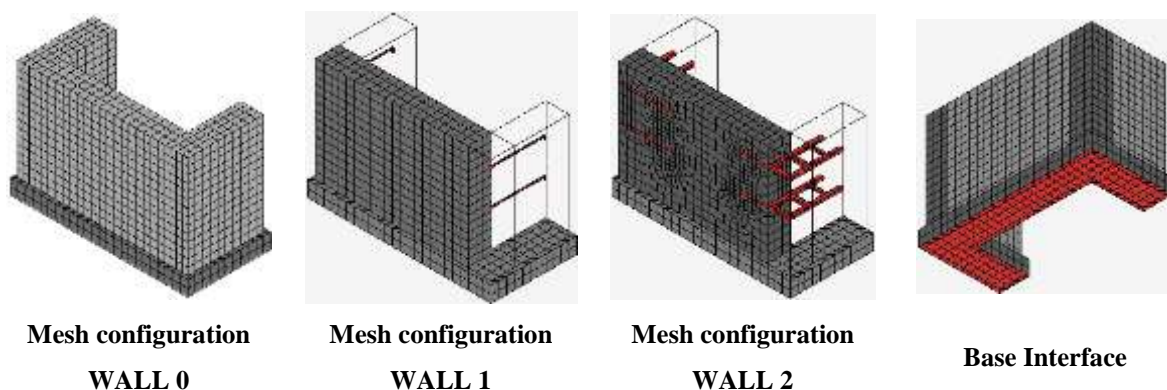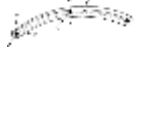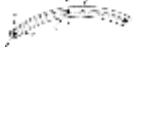
Figure 6. Reference models and embedded reinforcing elements; interface elements used at the reinforced concrete base (right)

In modelling approach 1, steel and timber reinforcing elements were modelled using

tetrahedron solid 3D elements (CHX60). The embedded steel and timber elements are considered to be perfectly connected with the wall. Hence, common nodes share all degrees of freedom and no interface elements are used.

The same criteria have been applied in modelling approach 2; the only difference is represented by the element used to define the embedded reinforcements, namely three-node 3D beam element (CL18B). Table 3 summarizes the aforementioned strategies.

	WALL 0		WALL 1		WALL 2	
	Approach 1	Approach 2	Approach 1	Approach 2	Approach 1	Approach 2
MASONRY	CHX60		CHX60		CHX60	
STEEL REINFOR.	-	-	CHX60	CL18B	CHX60	CL18B
TIMBER REINFOR.	-	-	CHX60	CL18B	CHX60	CL18B
FLOOR INTERAFCE	CQ48I		CQ48I		CQ48I	

Table 3. Modelling approaches summary

3.2. Calibration of the numerical model

Firstly, reference material elastic properties were estimated based on the results of the sonic tests (Table 1). Successively (2), an adjustment of the properties based on the comparison between the numerical and experimental frequencies was carried out. Finally, (3) the nonlinear material properties were adjusted based on the comparison of the force displacement envelope obtained in the out-of-plane experimental test with the nonlinear static (pushover) analysis performed on the numerical model. Moreover, changes in interface elastic properties allowed to obtain values of natural frequencies and mode shapes compatible with the experimental results. A preliminary pushover analysis was carried out to further adjust the mechanical properties according to the guidelines proposed in [3] and [15]. Table 4 summarizes the values obtained both for linear and nonlinear properties.

|	Linear Material Properties			Non-linear material properties			
	E (MPa)	ν	ρ (kg/m^3)	fc (MPa)	Gfc (N/m)	ft (MPa)	Gf1 (N/m)
WALL 0	3600	0.39	2495	3.60	5760	0.07	12
WALL 1	2450	0.28	2513	2.45	3917	0.07	12
WALL 2	2974	0.25	2482	2.97	4760	0.07	12

Table 4. Linear and non-linear material properties after calibration procedure
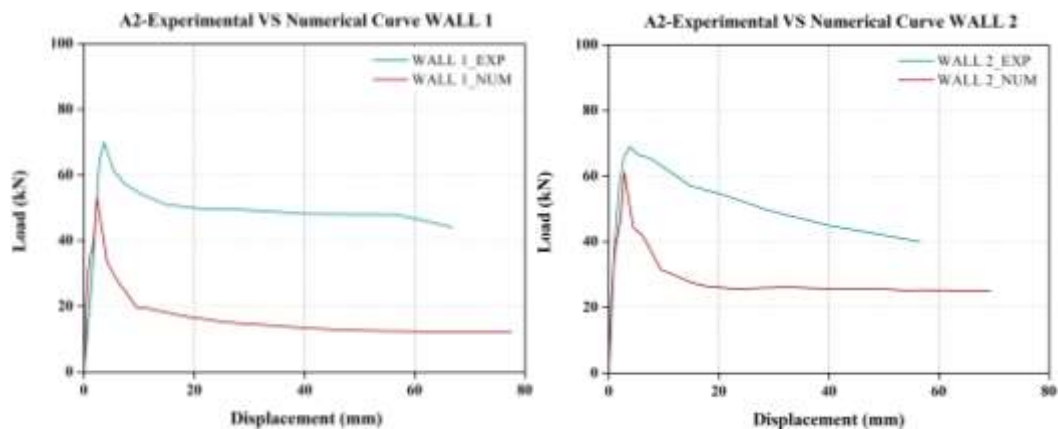
3.3. Numerical VS Experimental results

The numerical model was analysed by means of nonlinear static (pushover) analysis, considering the boundary and loading conditions adopted in the experimental tests. The vertical actions applied to the model were the self-weight of the structure and the additional uniformly distributed load on the transversal walls, which was equal to 10 kN on each side in WALL 1. A value of 20 kN was considered in WALL 2 in order to take into account some variations in terms of load distribution detected during the test. A uniformly distributed horizontal load, simulating the airbag action during the OOP test, was applied on the rear surface of the frontal wall. The pushover analysis consists in the incremental application of the aforementioned horizontal load until collapse.

The results of the push-over analysis is a capacity curve, which represents the horizontal load versus the control point displacement taken at the same position where the control LVDT was placed during the experimental test (top mid-span of the frontal wall).

Therefore, the push-over curve can be directly compared with the experimental force-displacement envelope. Figure 7 and Figure 8 show a comparison between numerical curve and experimental envelope using modelling approach 1 and modelling approach 2 respectively.
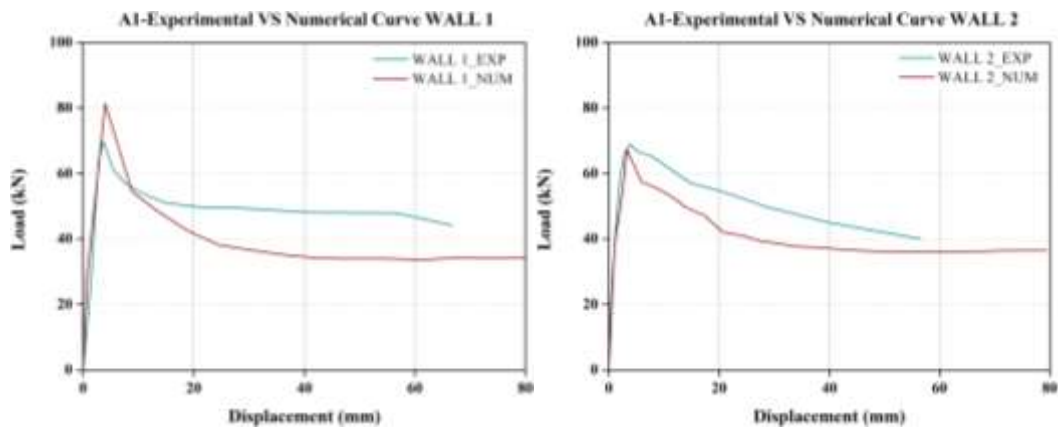
Figure 7. Approach 1 – Experimental VS Numerical capacity curve (WALL 1, WALL 2)

Figure 8. Approach 2 – Experimental VS Numerical capacity curve (WALL 1, WALL 2)

Capacity curves related to modelling approach 1 highlight a linear behaviour, which accurately reproduce the experimental results in both WALL 1 and WALL 2. Moreover, WALL 2 post-peak numerical branch is closer to the trend characterizing the experimental envelop, if compared to WALL 1 curve, meaning that the behaviour of the masonry prototype represents a global response closer to the "ideal" one.

In modelling approach 2, peak load and post-peak behaviour appear to be understated if compared both to the experimental results and to the numerical results regarding modelling approach 1.
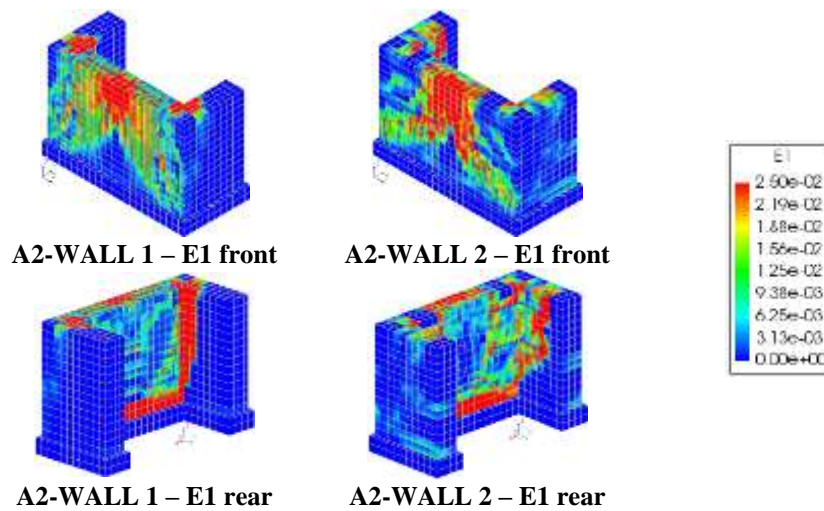
Looking at Figure 7 (approach 1), it is clear that WALL 1 maximum load is around 16% higher than the experimental result (81.43 kN against 69.91 kN). Conversely, numerical peak load in WALL 2 is 2% lower than the experimental load (67.50 kN against 68.91 kN).

In Figure 8 (approach 2), WALL 1 numerical peak load is around 31% lower than the experimental results (53.27 kN against 69.91 kN); a similar trend is detectable in WALL 2 even though numerical peak load is only 13% lower than the experimental one (61.18 kN against 68.91 kN).

Figure 9 and Figure 10 depict the maximum principal strain (E1) distribution, related to a displacement level of 40 mm, resulted from the analyses based on modelling approach 1 and modelling approach 2 respectively.

A1-WALL 1 – E1 front   **A1-WALL 2 – E1 front**

A1-WALL 1 – E1 rear   **A1-WALL 2 – E1 rear**
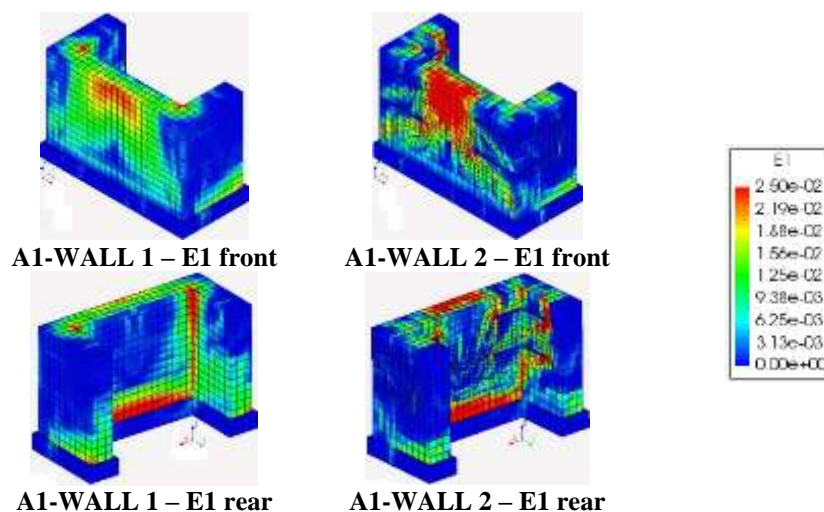
Figure 9. Approach 1 – Maximum principal strain distribution (E1)

| A2-WALL 1 – E1 front | A2-WALL 2 – E1 front |
| A2-WALL 1 – E1 rear | A2-WALL 2 – E1 rear |

Figure 10. Approach 2 – Maximum principal strain distribution (E1)

Overall, it is possible to say that the strain distribution is similar in both modelling approaches, the most damaged areas of the models correspond to the inner corners and to the central upper part of the main façade, consistenly also with the crack pattern resulted after the out-of-plane test (see Figure 5).

It is also interesting to point out that, despite the lower peak loads attained in modelling approach 2, the strain concentration at the inner corners and at the base of the numerical model appears to be higher if compared to the outcomes related to approach 1.

Furthermore, strain concentration at the base of the lateral walls is also detectable in modelling approach 1 (both in WALL 1 and WALL 2), whereas it is negligible in modelling approach 2. Hence, the rocking machanism of both walls is better captured when modelling approach 1 is applied.

4. CONCLUSIONS

This paper present a comparison between two different modellin strategies aiming at the simulation of out-of-plane tests carried out on reinforced stone masonry walls. In modelling approach 1, embedded steel and timber reinforcemend have been modelled using solid elements (CHX60), whereas 3D beams elements(CL18B) have been utlized with the same purpose in modelling approach 2. The capacity curves obtained by means of push-over analyses showed a good approximation of the linear elastic behaviour, but the peak loads related to the approach 2 were understated if compared both to the experimental results and to the numerical results of modelling approach 1.

Additionally, the strain distribution related to modelling approach 1, proved to be more consistent with the experimental results; the failure mechanisms characterizing the out-of-plane tests appear to be better simulated.

Overall, despite the computational efforts characterizing modelling approach 1 is more significant if compared to the second strategy, it is possible to say that it effectvely captured the global behaviour of the tested protoypes in terms of maximu loads attained predicting, in an accurate way damage distribution both in WALL 1 and WALL 2.

Table 5 summarizes the main outcomes of the analyses carried out applying both approach 1 and approach 2.
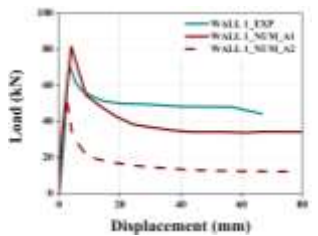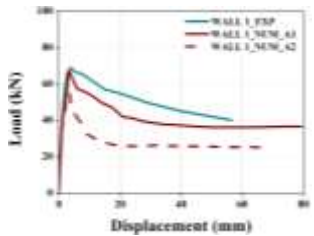
	EXP. PEAK LOAD	NUM. PEAK LOAD		CAPACITY CURVES	
		Approach 1	Approach 2	WALL 1	WALL 2
WALL 1	69.91 kN	81.43 kN (+16%)	67.50 kN (-2%)		
WALL 2	68.91 kN	53.27 kN (-31%)	61.18 kN (-13%)		

Table 5. Summary of experimental and numerical results

5. REFERENCES

[1] B. Helly, «Local seismic cultures: a European research program for the protection of traditional housing stock,» *Annals of Geophysics,* pp. 791-794, November-December 1995.

[2] R. Langenbach, «From "Opus Craticium" to the "Chicago Frame": Earthquake-Resistant Traditional Construction,» *International Journal of Architectural Heritage,* pp. 29-59, May 2007.

[3] M. Tomazevic, Earthquake-Resistant Design of Masonry Buildings, London: Imperial College Press, 1999.

[4] K. T. Doherty, *PhD Thesis,* Adelaide: Department of Civil and Environmental Engineering, 2000.

[5] D. D'Ayala, Y. Shi e C. Stammers, «Dynamic multi-body behaviour of historic masonry buildings models,» in *Structural Analysis of Historic Construction*, London, 2008.

[6] O. Al Shawa, L. Sorrentino e D. Liberatore, «Simulation Of Shake Table Tests on Out-of-Plane Masonry Buildings. Part (II): Combined Finite-Discrete Elements,» *International Journal of Architectural Heritage,* pp. 79-93, November 2016.

[7] Candeias, C. Costa, Mendes, Costa e Lourenço, «Experimental Assessment of the Out-of-Plane Performance of Masonry Buildings Through Shaking Table Tests,» *International Journal of Architectural Heritage,* pp. 31-58, December 2016.

[8] P. Roca, M. Cervera, G. Gariup e L. Pelà, «Structural Analysis of Masonry Historical Constructions - Classical and Advanced Approaches,» *Arch Comput Methods Eng,* 299-325 July 2010.

[9] T. M. Ferreira, A. Costa e A. Costa, «Analysis of the Out-Of-Plane Seismic Behavior of Unreinforced Masonry: A Literature Review,» *International Journal of Architectural Heritage,* pp. 949-972, November 2014.

[10] H. Maccarni, G. Vasconcelos, H. Rodrigues, J. Ortega e P. B. Lourenço, «Out-of-plane behavior of stone masonry walls: Experimental and numerical analysis,» *Construction and Building Materials,* pp. 430-452, 2018.

[11] L. Martins, G. Vasconcelos, J. Ortega, P. Lourenço, H. Rodrigue, L. Silva e C. Palha, «Characterization of dry stone walls to out-of plane actions,» in *10th Congresso*

Nacional de Mecânica Experimental, Lisbon, 2016.

[12] DIANA - Finite Element Analysis , DIsplacement method ANalizer. User's Manual, release 10.2, Delft, The Netherlands: DIANA FEA BV , 2017.

[13] P. B. Lourenço, «Masonry Modeling,» in *Encyclopedia of Earthquake Engineering*, Berlin, Springer Berlin Heidelberg, 2015, pp. 1-13.

[14] P. B. Lourennço e J. M. Pereira, «Seismic Retrofitting Project: Recommendations for Advanced Modeling of Historic Earthen Sites,» The Getty Conservation Institute, Los Angeles, 2018.

[15] P. Lourenço, «Recent advances in Masonry modelling: micromodelling and homogenisation,» in *Multiscale Modeling in Solid Mechanics: Computational Approaches*, London, Imperial College Press, 2009, pp. 251-294.